HAL
open science

The Inhibitor Thiomandelic Acid Binds to Both Metal Ions in Metallo-β-lactamase and Induces Positive Cooperativity in Metal Binding

Christian Damblon, Mikael Jensen, Abdessamad Ababou, Igor Barsukov, Cyril Papamicaël, Christopher J Schofield, Lars Olsen, Rogert Bauer, Gordon C.K. Roberts

To cite this version:

Christian Damblon, Mikael Jensen, Abdessamad Ababou, Igor Barsukov, Cyril Papamicaël, et al.. The Inhibitor Thiomandelic Acid Binds to Both Metal Ions in Metallo-β-lactamase and Induces Positive Cooperativity in Metal Binding. Journal of Biological Chemistry, 2003, 278 (31), pp.29240-29251. 10.1074/jbc.M301562200 . hal-03856336

HAL Id: hal-03856336

https://hal.science/hal-03856336v1

Submitted on 16 Nov 2022

HAL is a multi-disciplinary open access archive for the deposit and dissemination of scientific research documents, whether they are published or not. The documents may come from teaching and research institutions in France or abroad, or from public or private research centers.

L'archive ouverte pluridisciplinaire **HAL**, est destinée au dépôt et à la diffusion de documents scientifiques de niveau recherche, publiés ou non, émanant des établissements d'enseignement et de recherche français ou étrangers, des laboratoires publics ou privés.

THE JOURNAL OF BIOLOGICAL CHEMISTRY
Vol. 278, No. 31, Issue of August 1, pp. 29240–29251, 2003
Printed in U.S.A.
© 2003 by The American Society for Biochemistry and Molecular Biology, Inc.

The Inhibitor Thiomandelic Acid Binds to Both Metal Ions in Metallo-β-lactamase and Induces Positive Cooperativity in Metal Binding*[S]

Received for publication, February 13, 2003, and in revised form, April 28, 2003
Published, JBC Papers in Press, April 29, 2003, DOI 10.1074/jbc.M301562200

Christian Damblon‡, Mikael Jensen§, Abdessamad Ababou‡, Igor Barsukov‡, Cyril Papamicael¶, Christopher J. Schofield¶, Lars Olsen§, Rogert Bauer§, and Gordon C. K. Roberts‡‖

From the ‡Biological NMR Centre, Department of Biochemistry, University of Leicester, P.O. Box 138, University Road, Leicester LE1 9HN, United Kingdom, the §Department of Mathematics and Physics, The Royal Veterinary and Agricultural University, Thorvaldsensvej 40, DK-1871 Frederiksberg C, Denmark, and ¶The Oxford Centre for Molecular Sciences and The Dyson Perrins Laboratory, South Parks Road, Oxford OX1 3QY, United Kingdom

Thiomandelic acid is a simple, broad spectrum, and reasonably potent inhibitor of metallo-β-lactamases, enzymes that mediate resistance to β-lactam antibiotics. We report studies by NMR and perturbed angular correlation (PAC) spectroscopy of the mode of binding of the *R* and *S* enantiomers of thiomandelic acid, focusing on their interaction with the two metal ions in cadmium-substituted *Bacillus cereus* metallo-β-lactamase. The ^{113}Cd resonances are specifically assigned to the metals in the two individual sites on the protein by using ^{113}Cd-edited ^{1}H NMR spectra. Each enantiomer of thiomandelate produces large downfield shifts of both ^{113}Cd resonances and changes in the PAC spectra, which indicate that they bind such that the thiol of the inhibitor bridges between the two metals. For *R*-thiomandelate, this is unambiguously confirmed by the observation of scalar coupling between Hα of the inhibitor and both cadmium ions. The NMR and PAC spectra reveal that the two chiral forms of the inhibitor differ in the details of their coordination geometry. The complex with *R*-thiomandelate, but not that with the *S*-enantiomer, shows evidence in the PAC spectra of a dynamic process in the nanosecond time regime, the possible nature of which is discussed. The thiomandelate complex of the mononuclear enzyme can be detected only at low metal to enzyme stoichiometry; the relative populations of mononuclear and binuclear enzyme as a function of cadmium concentration provide clear evidence for positive cooperativity in metal ion binding in the presence of the inhibitor, in contrast to the negative cooperativity observed in the free enzyme.

β-Lactamases inactivate β-lactam antibiotics by catalyzing the hydrolysis of their endocyclic amide bond and play a major role in the emergence of strains of pathogenic bacteria resistant to these important antibiotics (1). The β-lactamases that contain a nucleophilic serine side chain as a key component of their active site (classes A, C, and D) have been extensively studied due to their established clinical importance. The class B β-lactamases or metallo-β-lactamases (MBLs)[1] are metalloproteins that require one or two zinc ion(s) for their activity (2) and are less well understood. The first of these enzymes to be discovered was produced by an innocuous strain of *Bacillus cereus* (3), but in the last 20 years, MBL-mediated resistance has appeared in several pathogenic strains and is being rapidly spread by horizontal transfer, involving both plasmid- and integron-borne genetic elements (4, 5).

The structures of several MBLs have been solved by x-ray diffraction and reveal two potential zinc ion binding sites at the active site (6–16). The zinc ligands are not fully conserved between the different subclasses of MBL. In the subclass B1 enzymes, such as the *B. cereus* enzyme BcII, which is the subject of the present work, the zinc in site 1 is coordinated by the imidazole rings of three histidine residues (86, 88, and 149 in the *B. cereus* enzyme or 116, 118, and 196 using the class B β-lactamase (BBL) numbering (17), given in parentheses henceforth) and a solvent molecule. In site 2, the metal is coordinated by a histidine (210, BBL263), an aspartic acid (90, BBL120), a cysteine (168, BBL221), and one or two solvent molecules. The two metal ions are relatively close to each other, but the apparent distance between them ranges from 3.4 to 4.4 Å in different structures of the BcII and CcrA (*Bacteroides fragilis*) enzymes (8–11, 13, 15, 16). Several structures of the CcrA enzyme show a bridging ligand (9, 11, 13) between the two metals, suggested to be an hydroxide ion; however, a bridging solvent molecule is not universally present in structures of this enzyme (7, 14). In a structure of BcII containing two zinc ions determined at pH 7.5, a similar bridging solvent molecule is seen (15), but in structures of this enzyme at lower pH, this solvent molecule is much more closely associated to the zinc in site 1 than to that in site 2 (8, 10). The second solvent molecule at site 2 is carbonate (8) or water (7, 9–11, 13) but is missing in one structure (15) (as well as in structures with inhibitors bound) (14, 16). The coordination of the metal ions is thus quite variable, perhaps contributing to some of the observed differences in substrate profiles and zinc affinities among MBLs (18–20). The bridging hydroxide ion or water molecule has been proposed to be the nucleophile responsible for β-lactam hydrolysis, but the precise role of the two metals in catalysis remains unclear; mechanisms have been proposed in which

* This work was supported by Biotechnology and Biological Sciences Research Council Grant 91/BI3539, by European Union TMR Network Grant CT 98-0232, and by the Danish Research Council for Natural Sciences. The costs of publication of this article were defrayed in part by the payment of page charges. This article must therefore be hereby marked "*advertisement*" in accordance with 18 U.S.C. Section 1734 solely to indicate this fact.

[S] The on-line version of this article (available at http://www.jbc.org) contains an additional figure.

‖ To whom correspondence should be addressed. Tel.: 44-116-252-2978; Fax: 44-116-223-1503; E-mail gcr@le.ac.uk.

[1] The abbreviations used are: MBL, metallo-β-lactamase; BBL, class B β-lactamase; MES, 4-morpholinoethanesulfonic acid; NQI, nuclear quadrupole interaction; AOM, angular overlap model.

This is an Open Access article under the CC BY license.

This paper is available on line at http://www.jbc.org

only site I plays a direct role in catalysis (21) or in which the two zinc ions are both involved as a binuclear center (2, 12, 20). The BcII enzyme is active with either one or two zinc ions bound, however, with different kinetic characteristics (15, 22).[2]

Inhibitors of the class A serine β-lactamases, such as clavulanic acid, have been very widely used to protect penicillins from β-lactamase-mediated hydrolysis. However, since MBLs are resistant to all clinically used serine β-lactamase inactivators, the search for a clinically useful inhibitor of MBLs remains an important objective. We have recently reported (23) that thiomandelic acid (α-mercaptophenylacetic acid) is a broad spectrum and reasonably potent inhibitor of MBLs. Structure-activity relationships show that the thiol is essential for activity, and it was postulated that the inhibitor thiol binds to the zinc ions. We now report direct studies of the interaction of thiomandelate with the active site metals in cadmium-substituted *B. cereus* MBL. In the majority of MBLs, zinc can be exchanged with cadmium to yield catalytically active enzymes (15), and in the case of CcrA the structure of the cadmium-substituted enzyme has been shown to be essentially identical to that of the zinc enzyme (13). Isotopes of cadmium provide very convenient probes for NMR and PAC spectroscopy, allowing direct studies of the coordination and dynamics of the metal ion. We have reported the use of a combination of NMR and PAC spectroscopy to study cadmium binding to *B. cereus* MBL, revealing rapid intramolecular exchange of the metal between the two sites in the monocadmium enzyme and negative cooperativity in metal binding (24). We have now used a similar combination of ^{1}H, ^{15}N, and ^{113}Cd NMR and ^{111m}Cd PAC spectroscopy to study the interaction of the *R* and *S* forms of thiomandelate with the metal ions in cadmium-substituted *B. cereus* MBL.

EXPERIMENTAL PROCEDURES

Materials—^{15}N-Labeled protein was expressed from plasmid pET/BCII in *E. coli* BL21(DE3). Cells were grown at 30 °C in M9 minimal medium with 4 g of glucose and 1 g of $^{15}NH_4Cl$ as the only nitrogen source. Expression was induced by adding 0.5 mM isopropyl-β-thiogalactoside when the culture had an absorbance at 600 nm of 1.25. After 16 h, the cells were harvested by centrifugation and broken by sonication, and the β-lactamase was purified as described elsewhere (6, 25) and converted to apoenzyme according to Paul-Soto *et al.* (22). *R*- and *S*-thiomandelic acid were synthesized as described earlier (23).

NMR Spectroscopy—For the NMR studies, the cadmium enzyme was prepared at room temperature, by adding gradually a small volume (1–10 μl) of 0.1 M $^{113}CdCl_2$ (95.83% enriched) to the β-lactamase apoenzyme (0.8–1.8 mM) in 10 mM MES-Na, 100 mM NaCl, pH 6.4, 5% $^{2}H_2O$ to give [cadmium]/[enzyme] ratios of 1.0–2.0. Samples of the inhibitor complexes were prepared by the addition of microliter volumes of stock inhibitor solution (50 mM in 0.5 M MES buffer, 100 mM NaCl, pH 6.4) to the enzyme solution. The final sample volume was 450 μl, and the temperature during acquisition was 298 K. The same enzyme preparation and similar sample preparation procedures were used in PAC spectroscopy (see below).

All NMR experiments were performed on Bruker Avance DRX/DMX instruments. ^{1}H spectra were obtained at 600 MHz by using a water-flip-back pulse combined with Watergate (26, 27). Backbone NH resonances were observed by ^{1}H,^{15}N heteronuclear single quantum coherence (HSQC) with States-TPPI and Watergate. Observation of imidazole ^{15}N(C)H resonances was by ^{1}H,^{15}N HMQC (heteronuclear multiple quantum coherence) with a refocusing delay of 16.7 ms ($1/2J_{N(C)H}$), as described previously (25). The same pulse sequence was used for ^{1}H,^{113}Cd HMQC with 10, 16.7, or 33.3 ms ($1/2J_{Cd\text{-}H}$) as refocusing delay. Selective decoupling experiments were performed using G3 Gaussian cascade shaped pulses within an MLEV sequence (28). All ^{113}Cd experiments were performed at 133 MHz. The external reference was $Cd(ClO_4)_2$. For the direct detection of ^{113}Cd, 100,000 free induction decays were recorded, acquiring 4096 complex points in 51 ms, with a 30° observe pulse (4 μs), a spectral width of 80,000 Hz (600 ppm), and a relaxation delay of 0.5 s. A 200-Hz exponential multiplication was used prior to Fourier transformation, followed by base-line correction.

PAC Spectroscopy—The necessary amounts of the nuclear probe ^{111m}Cd (49-min half-life) were produced by a 24-MeV α particle bombardment of 98.9% enriched metallic ^{108}Pd (Oak Ridge National Laboratory). The radiochemical separation of the target and the purification of ^{111m}Cd have been described previously (29). The resulting carrier-free solution (50 μl) was split in two with volume ratios of 1:4, allowing two consecutive PAC counting sessions with equal statistics to be performed from one ^{111m}Cd production batch. The tracer solution for each experiment was subsequently adjusted to the desired cadmium concentration by the addition of small volumes of $CdCl_2$ solution in metal-depleted MES buffer. The added amounts of cadmium (0.25–190 nmol) were large compared with both the ^{111m}Cd content and other contaminating metals in the solution, even at the lowest concentrations used ([Cd]/[enzyme] = 0.01). Control experiments indicated that any zinc contamination was <0.005 molar equivalent. The apoenzyme was added, giving a final enzyme concentration of 0.5 mM in the PAC samples. The pH was adjusted to pH 7.0 (room temperature) by the addition of small amounts of 1–5 M HCl or NaOH. The final sample conditions were 50 mM HEPES, 130 mM NaCl, with volumes ranging from 50 to 200 μl. After a 10-min waiting period at room temperature, to ensure equilibrium for metal binding to the enzyme, pure crystalline sucrose (ACS reagent from Sigma) was added to give a 55% (w/w) solution in order to slow the rotational diffusion of the enzyme. The PAC sample preparation (tracer and metal addition, incubation, pH adjustment, and sucrose addition) was done immediately before each measurement, allowing a direct transfer of the sample to the temperature-controlled environment of the PAC sample holder. Unless otherwise noted, PAC experiments were performed at 1 °C.

The differential time PAC spectrometer (30) uses six 2″ BaF_2 scintillation detectors located in a face-centered cube around the sample to absorb the 151 + 245-keV γ-cascade of the ^{111m}Cd decay. The FWHM time resolution of the instrument is 1.0 ns, the single detector count rate is ~60 kcps, and the total data acquisition lasts 100–200 min, giving 50–100 million recorded coincidences.

PAC Data Analysis—The perturbation function, $G_2(t)$, of the angular correlation pattern is derived from the measurements as described previously (29–32). This function depends on the local electric quadrupole interaction at the site of the cadmium nucleus and contains the structural information about the co-ordination geometry that can be deduced from a PAC experiment. In the case of identical, static, and randomly oriented molecules, the perturbation function denoted $G_2(t)$ can be expressed as follows,

$$G_2(t) = a_0 + a_1 \cos(\omega_1 t) + a_2 \cos(\omega_2 t) + a_3 \cos(\omega_3 t) \qquad \text{(Eq. 1)}$$

where ω_1, ω_2, and ω_3 represent the three difference frequencies proportional to the energy difference between the three sublevels of the spin 5/2 intermediate state of the cadmium nucleus (32). Note that $\omega_1 + \omega_2 = \omega_3$. The perturbation function was Fourier transformed as described in Bauer *et al.* (30). The Fourier transform of $G_2(t)$ exhibits three frequencies for each type of environment in the enzyme, giving rise to a nuclear quadrupole interaction (NQI). Each NQI can theoretically be described by the parameters ω_0 and η. The relation between the two parameters ω_0 and η and the frequencies and amplitudes in the expression for $G_2(t)$ can be found in Bauer (32). Thus, ω_0 and η, which are related to the coordination geometry of the cadmium ion, can be determined from the time dependence of $G_2(t)$.

In the liquid state, the NQI in itself is time-dependent because of the Brownian motion of the protein, giving an exponential damping of the observed correlation pattern with a time constant equal to the rotational diffusion time τ_R. Additional time-dependent variation in the local NQIs can be induced by, for example, an exchange process between two coordination geometries. A distribution of coordination geometries is allowed for by introducing a Gaussian frequency spread $\delta = \Delta\omega_0/\omega_0$. The perturbation function $A_2G_2(t)$, where A_2 is the amplitude, was analyzed by a conventional nonlinear least-squares fitting routine, giving the frequency ω_0, the asymmetry η, the relative Gaussian frequency distribution δ, and the rotational diffusion time τ_R for each of the observed NQIs.

In all cases where more than a single NQI is observed, the perturbation function is assumed to be the sum of the individual perturbation functions weighted by a population factor (30). However, the fitting procedure will not always succeed in giving all five parameters for each of several NQIs in a given spectrum. Additional constraints are added to assist the fitting in these cases. In the case of experiments with *S*-thiomandelate, it was possible (judged by acceptable values for the reduced χ^2 function) to fit the spectra obtained at different [cadmium]/

[2] C. Damblon, V. Nandwani, and G. C. K. Roberts, unpublished data.

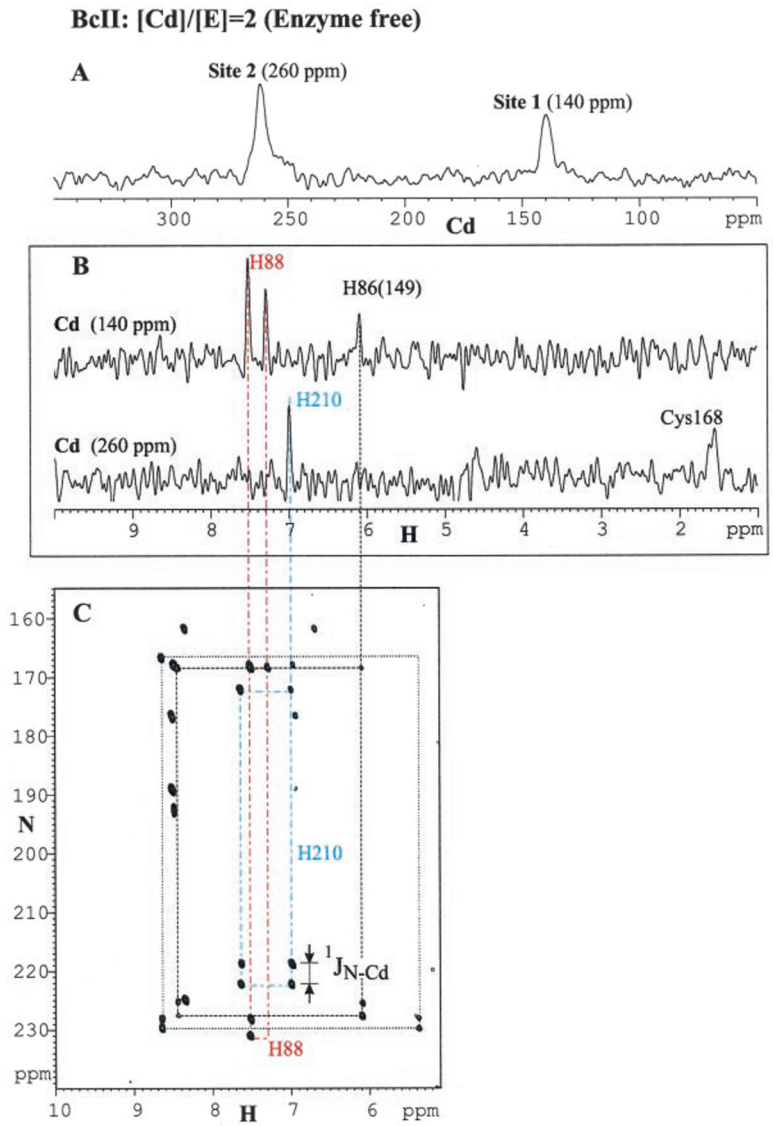

FIG. 1. **NMR spectra of ^{113}Cd-substituted BcII enzyme.** *A*, ^{113}Cd spectrum, showing the resonances of the cadmium ions in sites 1 and 2. *B*, ^{113}Cd-edited ^{1}H spectra, showing the resonances of protons scalar coupled to the two individual ^{113}Cd nuclei. *C*, ^{1}H-^{15}N HMQC spectrum of the imidazole groups, showing the connectivities that allow the assignment of the imidazole ^{1}H resonances in *B*. The four cadmium-bound imidazoles are identified by the splitting observed in the ^{15}N dimension arising from the $^{1}J_{\text{N-Cd}}$ coupling.

[enzyme] ratios simultaneously. This global fit gave four distinct NQIs, each having individual ω_0 and η values, but with identical values of τ_R and δ. Each *S*-thiomandelate measurement is assumed to contain these four NQIs with different amplitudes (possibly zero). The spectrum obtained at [cadmium]/[enzyme] = 1.9 must necessarily arise primarily from the binuclear enzyme, since no free cadmium is observed, with both sites almost equally populated, and it was thus fitted under the constraint of equal amplitude, and the amplitudes of the mononuclear NQIs were fixed to zero. The goodness of the fit was judged by the overall χ^2 value.

The fitting procedure was more complicated in the case of the spectra obtained in the presence of *R*-thiomandelate, where distinct dynamical features in the 1 °C spectrum prohibit an overall fit of all stoichiometries. The spectra of *R*-thiomandelate-inhibited samples at −20 °C and +30 °C were fitted assuming four NQIs, two of which are found and fitted at 30 °C and three at −20 °C. The temperature difference introduces differences in τ_R, and this parameter was not constrained in the fitting process. We assumed the same value of δ as found in the *S*-thiomandelate experiments in these fits.

Molecular Modeling—The starting point for the modeling was the crystal structure of the *B. cereus* enzyme containing two zinc atoms (8) (Protein Data Bank accession number 1bvt) with hydrogens added using the AMBER package (33) and the bicarbonate ion and water molecules coordinating the zinc ions removed; the charges were determined for all atoms using the program Divcon with a PM3 Hamiltonian coupled with a dielectric continuum model for the solvent effect (34, 35). The ligands *R*- and *S*-thiomandelate were built using AMBER, and the geometry optimization and charges determination were conducted using Divcon. Docking was carried with AutoDock (36), allowing flexibility about rotatable bonds of the inhibitor using the AutoTors utility but keeping the protein rigid. A large population size of 200 was used to ensure that conformational space was exhaustively searched; the maximum number of energy evaluations was set to 0.5 million (in tests, using 1 or 3 million did not improve the results), the number of trials was 200, the number of generations was 0.04 million, and all other parameters were set according to the defaults in the AutoDock manual (36). In additional test calculations, thiomandelate was docked into structures where Lys^{171} is in an extended conformation (see "Discussion"); the inhibitors were removed from the published structures, and the protein and ligand were parameterized as described by Hanessian *et al.* (37).

RESULTS

NMR Spectroscopy

Assignment of the ^{113}Cd Spectrum of Cadmium-substituted B. cereus MBL—As described earlier (24, 25), the BcII enzyme with two cadmium ions bound gives a ^{113}Cd NMR spectrum containing two distinct resonances at ~140 and ~260 ppm (Fig. 1*A*). These two signals have now been assigned to the two metal binding sites of the enzyme by means of ^{113}Cd-edited ^{1}H NMR spectra (Fig. 1*B*). The upfield ^{113}Cd resonance gives rise to three ^{1}H resonances in the region of the spectrum containing the imidazole H_δ and H_ϵ resonances of histidine residues, which can be identified by reference to the ^{1}H,^{15}N HSQC spectrum optimized for observation of these imidazole resonances

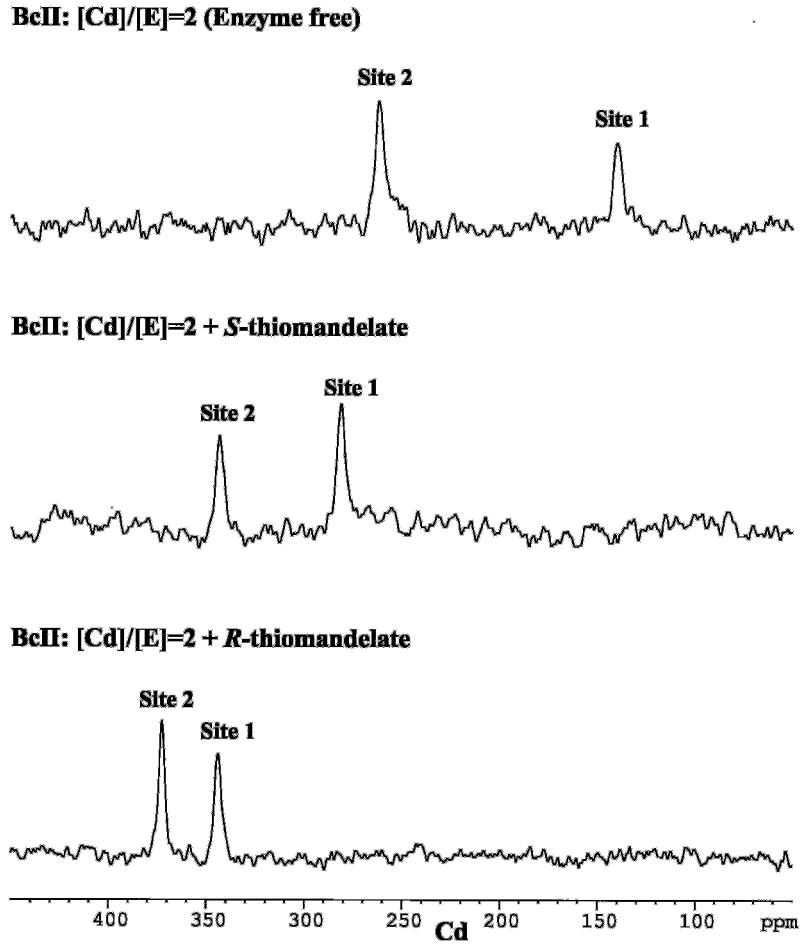

FIG. 2. **^{113}Cd NMR spectra of dicadmium BcII alone and in the presence of 1 equivalent of *R*-thiomandelate or *S*-thiomandelate.**

(25) shown in Fig. 1*C*. Two of these, at 7.3 and 7.5 ppm, can be assigned to His^{88} (BBL118) (25), the only metal-bound histidine that is in the $N_{\epsilon}H$ tautomeric form. The ^{113}Cd resonance at 140 ppm can thus be assigned to the metal in site 1, where it is coordinated by three histidine residues. Apart from the resonances of His^{88} (BBL118), another imidazole resonance, from His^{86} or His^{149} (BBL116 or BBL196), is observed at 6.1 ppm; the corresponding signal of the third histidine, at 5.4 ppm (25), is broad and is not observable in the ^{113}Cd-edited spectrum. The lower field ^{113}Cd resonance gives rise to one imidazole ^{1}H resonance, at 7.0 ppm, and one ^{1}H resonance in the aliphatic region, at 1.6 ppm; this ^{113}Cd signal can thus be assigned to the metal in site 2, the imidazole resonance being that of His^{210} (BBL263) (consistent with the results of studies of the zinc/cadmium hybrid enzyme[3] and the aliphatic resonance being that of one or both of the β-protons of Cys^{168} (BBL221).[4]

Effects of Thiomandelate Binding on the ^{113}Cd Spectrum—The addition of one molar equivalent of either *R*- or *S*-thiomandelate to the dicadmium enzyme leads to a substantial downfield shift of both of the ^{113}Cd resonances (Fig. 2). The addition of 0.5 molar equivalents of thiomandelate leads to a spectrum containing both resonances corresponding to the free enzyme and those corresponding to the complex, with approximately equal intensities, indicating that thiomandelate binding is in slow exchange on the ^{113}Cd NMR time scale. The further addition of the inhibitor from 1 to 2 molar equivalents does not change the NMR spectra. The direction and magnitude of the inhibitor-induced change in chemical shift is consistent with that expected for the coordination of a sulfur atom to each of the cadmium ions and hence with the idea that the inhibitors bind directly to both metal sites.

Direct evidence for this and the assignment of the two ^{113}Cd resonances in the inhibitor complexes can be obtained from ^{1}H,^{113}Cd HMQC spectra, shown for the *R*-thiomandelate complex in Fig. 3. Both the ^{113}Cd and the imidazole ^{1}H resonances of the inhibitor complexes are sharper than those of the free enzyme, and cross-peaks are observed from the 343 ppm ^{113}Cd resonance for three imidazoles, His^{88}, His^{86}, and His^{149} (BBL118, -116, and -196). (The latter two histidines have not been individually assigned in the cadmium-substituted enzyme but can be tentatively assigned, as shown in Table I, by comparison with the assigned resonances in the zinc enzyme (23).) The 343 ppm ^{113}Cd resonance can thus be unambiguously assigned to the cadmium in site 1. There is also a strong cross-peak to a signal at 5.36 ppm, which can be assigned to the CαH (benzylic proton) of the bound *R*-thiomandelate (chemical shift 4.72 ppm for the free inhibitor in $C^{2}HCl_{2}$). This inhibitor resonance also gives a strong cross-peak to the low field ^{113}Cd resonance (Fig. 3), which in turn shows cross-peaks to the imidazole protons of His^{210} (BBL263) and the β-proton(s) of Cys^{168} (BBL221) and can thus be assigned to the metal in site 2. The observation that, in a complex containing 1 molar equivalent of inhibitor, the *R*-thiomandelate resonance at 5.36 ppm gives a cross-peak in the ^{1}H,^{113}Cd HMQC spectrum to both ^{113}Cd resonances is clear evidence that *R*-thiomandelate coordinates through its sulfur atom to both cadmium ions.

This argument is further strengthened by detailed analysis

[3] C. Damblon and G. C. K. Roberts, manuscript in preparation.

[4] This resonance is assigned to the cysteine rather than to the aspartate in site 2, since the β-protons of the cysteine are separated from the ^{113}Cd by three bonds rather than the four in the case of the aspartate.

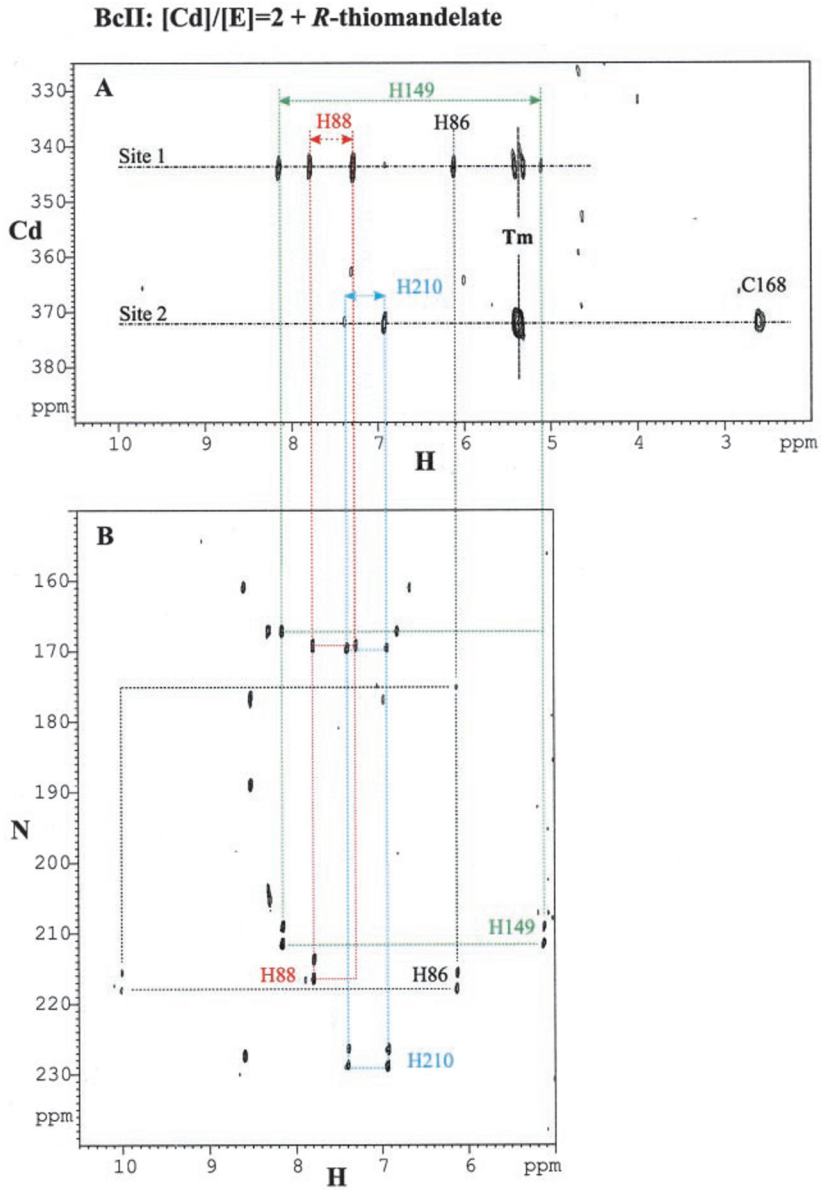

FIG. 3. **NMR spectra of dicadmium BcII in the presence of one equivalent of *R*-thiomandelate.** *A*, ^{1}H,^{113}Cd HMQC spectrum; *B*, ^{1}H,^{15}N HMQC spectrum of the imidazole resonances, allowing assignment of the imidazole cross-peaks in *A*.

of the resonance at 5.36 ppm in the ^{113}Cd-edited ^{1}H spectrum of the *R*-thiomandelate complex. This resonance is shown in Fig. 4, where it can be seen to consist of four lines. These could in principle arise from two doublets,[5] reflecting two separate thiomandelate-cadmium interactions, or a doublet of doublets, reflecting the simultaneous interaction of one thiomandelate with both cadmium ions; these two possibilities can be distinguished by ^{113}Cd decoupling experiments. Broadband ^{113}Cd decoupling gives rise to a single ^{1}H resonance, not the two separate resonances that would be predicted for two separate thiomandelate-cadmium interactions. Second, selective ^{113}Cd decoupling at 343 ppm leads to collapse of both the two outer pairs of lines, revealing a doublet of $^{3}J_{\text{H-Cd}}$ = 31 Hz, whereas selective decoupling at 372 ppm leads to collapse of the four-line pattern into a doublet of $^{3}J_{\text{H-Cd}}$ = 15 Hz. This behavior is exactly what would be predicted for a doublet of doublets arising from the interaction of one thiomandelate with both cadmium ions and provides unambiguous evidence that *R*-thiomandelate binds simultaneously to both cadmium ions in the enzyme. The 31-Hz $^{3}J_{\text{H-Cd}}$ scalar coupling can be assigned to the cadmium in site 2, and the 15-Hz scalar coupling can be assigned to the cadmium in site 1.

In the ^{1}H,^{113}Cd HMQC spectra of the *S*-thiomandelate complex (not shown), only a single correlation is observed for the ^{1}H resonance at 5.2 ppm assigned to the thiomandelate CαH, to the ^{113}Cd resonance at 375 ppm assigned to the cadmium in site 2, and the $^{3}J_{\text{H-Cd}}$ scalar couplings are clearly much smaller and are not resolved in spectra such as those in Fig. 4. In this case, there is a degree of ambiguity in the ^{1}H,^{113}Cd HMQC spectrum, since the imidazole resonance that appears at 5.2 ppm, upfield of the thiomandelate CαH signal, in the *R*-thiomandelate complex partly overlaps the latter signal in the *S*-thiomandelate complex. However, the similar downfield shifts of both the ^{113}Cd resonances on the binding of both isomers of the inhibitor, in particular the large downfield shift of the resonance of the cadmium in site 1, make it highly probable that the sulfur of *S*-thiomandelate, like that of *R*-thiomandelate, coordinates to both metals. The chemical shifts and scalar couplings to the metal ligands in the free enzyme and the two inhibitor complexes are summarized in Table I.

[5] Two thiomandelate CαH resonances with different chemical shifts, each split into a doublet by coupling to one ^{113}Cd; either two doublets of 31 Hz separated from one another by 0.113 ppm (15 Hz) or two doublets of 15 Hz separated from one another by 0.233 ppm (31 Hz).

TABLE I
Chemical shifts and scalar coupling constants for the cadmium ions and their ligands in B. cereus MBL, free and in complexes with R- and S-thiomandelate

Chemical shifts are shown in ppm, ^{113}Cd relative to $Cd[ClO_4]_2$, ^{1}H relative to DSS; scalar couplings are shown in Hertz, in italic type.

Complex	Free enzyme	Enzyme-*R*-thiomandelate	Enzyme-*S*-thiomandelate
^{113}Cd (site 1)	139.7	343.6	302.0
^{113}Cd (site 2)	261.7	372.4	356.2
His^{86b}			
N_δ, H_δ	169.0, 6.1	175.2, 6.1	177.5, 6.15
N_ε, H_ε, $^1J_{N\text{-}Cd}$	226.5, 8.4, *127*	216.8, 10.0, *142*	227.6, 9.65, *106*
His^{88}			
N_δ, H_δ, $^1J_{N\text{-}Cd}$	229.5, 7.3, *173*	215.0, 7.3, *165*	219.6, 7.73, *196*
N_ε, H_ε	168.5, 7.5	169.3, 7.8	170.0, 7.27
His^{149b}			
N_δ, H_δ	167.0, 5.4	167.2, 5.1	169.7, 5.15
N_ε, H_ε, $^1J_{N\text{-}Cd}$	228.9, 8.6, *96*	210.2, 8.1, *152*	216.5, 7.9, *170*
His^{210}			
N_δ, H_δ	172.4, 7.0	169.7, 6.9	170.1, 6.93
N_ε, H_ε, $^1J_{N\text{-}Cd}$	220.6, 7.6, *209*	227.7, 7.4, *145*	227.6, 7.3, *126*
Cys^{168}			
C_βH	1.55	2.6	2.71
Thiomandelate			
C_αH		5.36	5.12
$^3J_{H\text{-}Cd}$ (site 1)		*15*	
$^3J_{H\text{-}Cd}$ (site 2)		*31*	*<15*

[b] The connection between the resonances of His^{86} and His^{149} in the free enzyme and in the inhibitor complexes cannot yet be made unambiguously; the chemical shifts are listed so as to indicate the least shift difference between free enzyme and the complexes. The resonances of these two residues have not been individually assigned in the cadmium-substituted enzyme; the assignment shown is based on comparison (particularly of the Hδ and Hε chemical shifts) with the assigned resonances of the zinc enzyme (23).

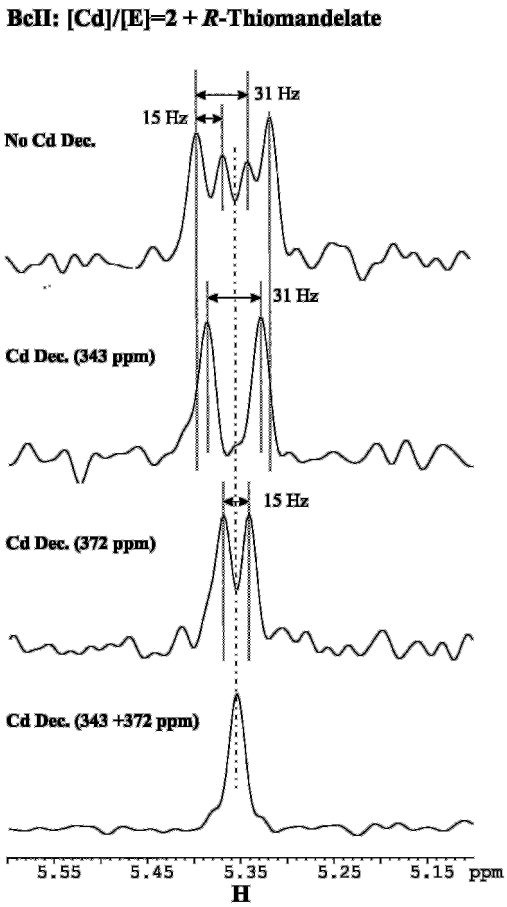

FIG. 4. **^{113}Cd-edited ^{1}H spectra of dicadmium BcII in the presence of 1 equivalent of *R*-thiomandelate.** The spectra show the multiplet assigned to CαH of thiomandelate with and without ^{113}Cd decoupling.

Thiomandelate Binding to the Monocadmium Enzyme—We have earlier reported that the ^{113}Cd spectrum of the enzyme having 1 cadmium equivalent bound contains a single resonance. Comparison with PAC spectra under identical conditions showed that this reflects a rapid intramolecular exchange of the single metal between the two sites (24). The addition of 1 molar equivalent of either *R*- or *S*-thiomandelate to the monocadmium enzyme led to a ^{113}Cd spectrum having two resonances at the same chemical shifts as those observed for the complexes of the dicadmium enzyme (Fig. 5). Furthermore, the ^{113}Cd-edited ^{1}H spectra of the *R*-thiomandelate complex showed that the thiomandelate CαH resonance at 5.35 ppm had the same ^{1}H,^{113}Cd scalar coupling as observed for the dicadmium enzyme (Fig. S1, Supplementary Material), demonstrating that the thiomandelate-enzyme complex contains two cadmium ions.

With this being the case, given that the overall [cadmium]/[enzyme] ratio is 1, the sample must also contain apoenzyme. This was confirmed by using the ^{1}H,^{15}N HSQC spectrum of the ^{15}N-labeled enzyme as a "fingerprint" of the different states of the enzyme (Fig. 6). It is clear that the spectrum of the sample containing enzyme, cadmium, and *R*-thiomandelate in a 1:1:1 ratio contains more amide cross-peaks in the HSQC spectrum than can be accounted for by the number of residues in the protein, indicating that this sample must consist of a mixture of species. Overlays with the spectrum of the apoenzyme (Fig. 6*A*) and with the spectrum of the *R*-thiomandelate complex of the dicadmium enzyme (Fig. 6*B*) show unequivocally that the sample contains a mixture of roughly equal amounts of these two species. All the resonances in the spectrum of the sample containing enzyme, cadmium, and *R*-thiomandelate in a 1:1:1 ratio can be accounted for by the sum of the spectra of apoenzyme and of the *R*-thiomandelate complex of the dicadmium enzyme.[6] No resonances were observed that could correspond to a thiomandelate complex of the monocadmium enzyme; we estimate that this complex would have been detected if it had been present at levels corresponding to ≥5% of the total enzyme.

[6] Three or four cross-peaks of the sample containing enzyme, cadmium, and *R*-thiomandelate in a 1:1:1 ratio show slight differences in chemical shift from the obviously corresponding cross-peaks in the spectrum of the apoenzyme. This can most probably be ascribed to slight differences in the conditions used for recording the two spectra.

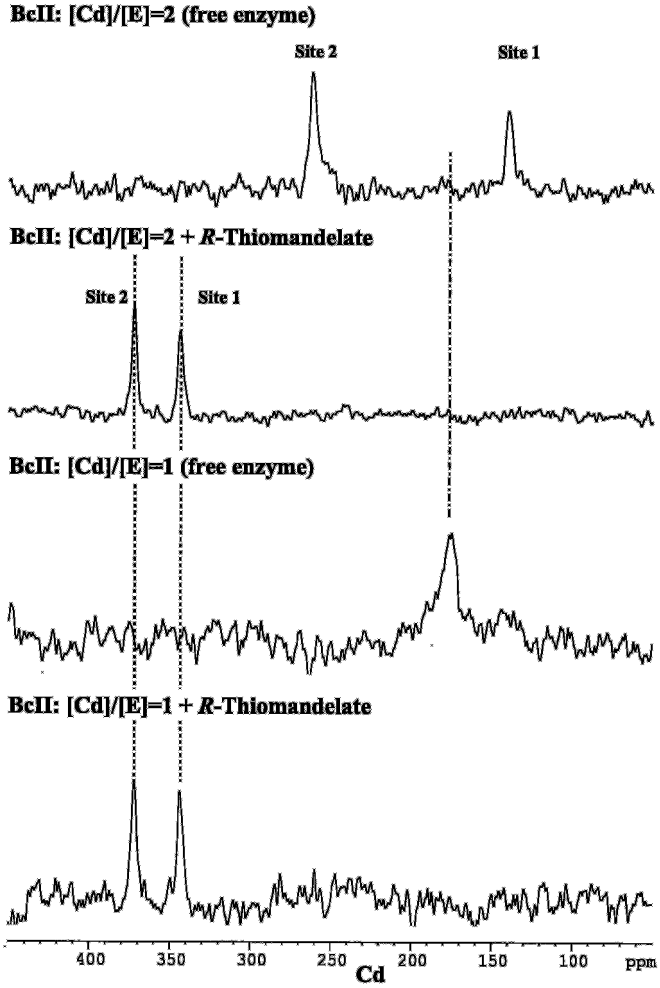

FIG. 5. **^{113}Cd spectra of dicadmium BcII and of monocadmium BcII with and without one equivalent of *R*-thiomandelate.**

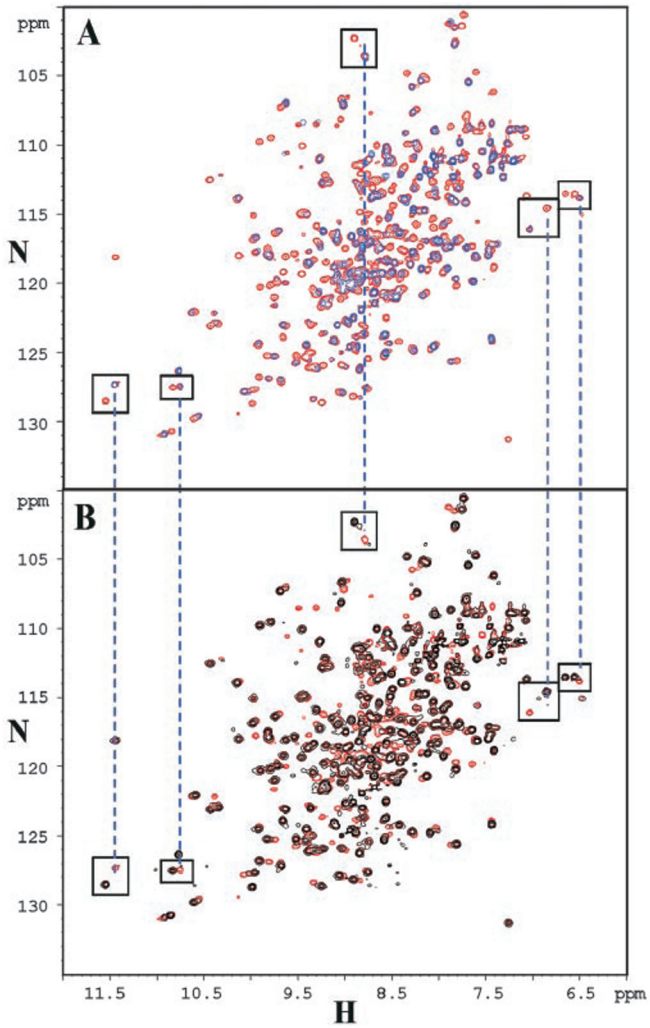

FIG. 6. **^{1}H,^{15}N HSQC spectra of the backbone amides of BcII.** *A*, comparison of spectra of monocadmium BcII with 1 equivalent of *R*-thiomandelate (*red*) and of BcII apoenzyme (*blue*). *B*, comparison of spectra of monocadmium BcII with 1 equivalent of *R*-thiomandelate (*red*) and of dicadmium BcII with 1 equivalent of *R*-thiomandelate (*black*).

These observations clearly demonstrate that the addition of thiomandelate to a sample of 1.8 mM enzyme containing cadmium at a [cadmium]/[enzyme] ratio of 1 leads to positive cooperativity in metal binding such that only the *R*-thiomandelate complex of the dicadmium enzyme (with a corresponding amount of apoenzyme) is observed. This is in marked contrast to the negative cooperativity in cadmium binding observed in the absence of inhibitor (24).

PAC Spectroscopy

The Enzyme-S-Thiomandelate Complex—Fig. 7 shows the Fourier transforms of PAC spectra recorded at different [Cd(II)]/[E] ratios in the presence of 1 molar equivalent of *S*-thiomandelate. The results of fitting the three spectra for this complex simultaneously, as described under "Experimental Procedures," are presented in Tables II and III. For the sample having [Cd(II)]/[E] = 1.9 and 1 molar equivalent of *S*-thiomandelate, both metal sites will be almost equally occupied, giving two NQIs of equal amplitude (NQI-1 and NQI-2 in Table II). Calculations using the angular overlap model (see "Discussion") suggest that NQI-1 corresponds to cadmium in site 2 and that NQI-2 corresponds to cadmium in site 1 and are consistent with the presence of a sulfur atom from the ligand in the coordination sphere of both metals. The presence of the peak at 0.26 gigarads/s at all stoichiometries shows that the binuclear cadmium enzyme must in fact be present in all cases. The substantial changes as a function of [cadmium]/[enzyme] at ~0.2 gigarads/s must reflect the presence of additional species, most likely monocadmium enzyme(s), at lower stoichiometries. This is reflected in the fitted parameters (Tables II and III), where a substantial proportion of NQI-4 is present at the lower stoichiometries (together with a small amount of NQI-3 at the lowest stoichiometry). However, from Table III it is clear that the binuclear species (NQI-1 and NQI-2) still predominates even at [Cd(II)]/[E] = 0.01, indicating cooperativity in metal ion binding.

The Enzyme-R-Thiomandelate Complex—The Fourier transforms of PAC spectra recorded at different [Cd(II)]/[enzyme] ratios in the presence of 1 molar equivalent of *R*-thiomandelate at 1 °C are shown in Fig. 8. In this case, the spectrum of the complex of the *R*-isomer at [Cd(II)]/[enzyme] = 1.9, which should be a simple spectrum with two NQIs at equal abundance, could not be satisfactorily fitted by the procedure used to analyze the corresponding spectrum of the complex of *S*-thiomandelate, since a reduced χ^2 sum of 1.9 was obtained. The most likely explanation of this failure to fit the spectrum with a simple model is the presence of dynamic features (in addition to rotational diffusion). PAC spectra of a sample containing enzyme, cadmium, and *R*-thiomandelate at a ratio of 1:1.9:1 were therefore obtained at temperatures of −20 and 30 °C (Fig. 9). These two spectra could be analyzed satisfactorily with three or two NQIs, respectively (Tables IV and V). In the

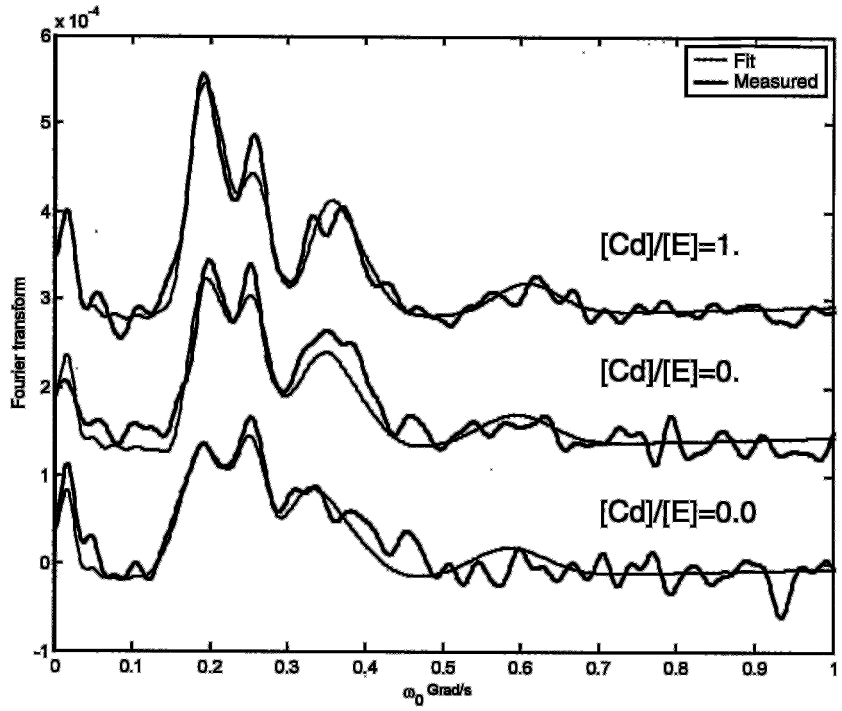

FIG. 7. **Effects of the addition of *S*-thiomandelate on the PAC spectra of BcII.** Spectra were recorded using 0.5 mM enzyme at 1 °C with [Cd(II)]/[enzyme] ratios of 0.01, 0.2, and 1.9 in the presence of 1 molar equivalent of *S*-thiomandelate. Fourier transforms of experimental PAC spectra are shown as *thick lines*, and corresponding fits are shown as *thin lines*.

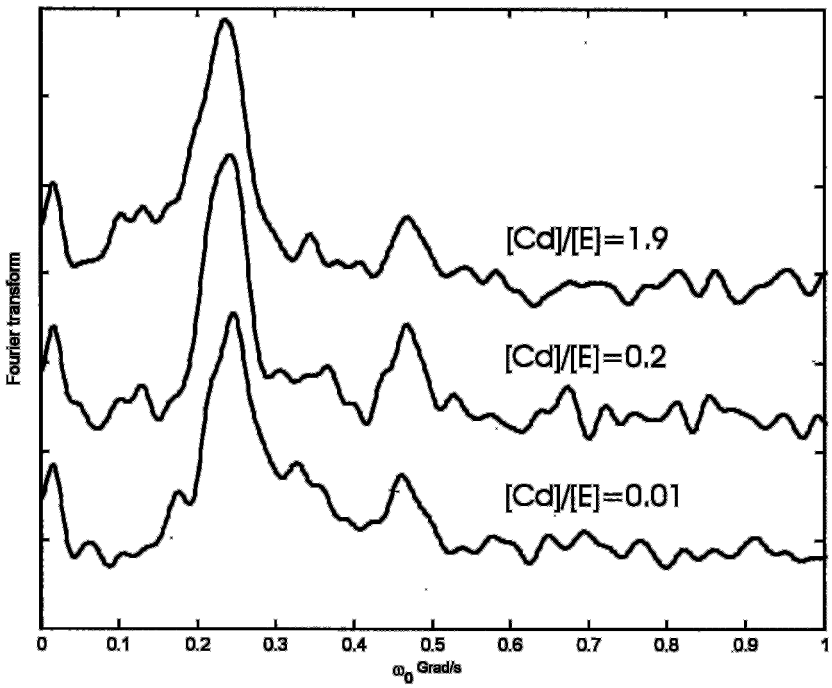

FIG. 8. **Effects of the addition of *R*-thiomandelate on the PAC spectra of BcII.** Spectra were recorded using 0.5 mM enzyme at 1 °C with [Cd(II)]/[enzyme] ratios of 0.01, 0.2, and 1.9 in the presence of 1 molar equivalent of *R*-thiomandelate.

spectrum obtained at −20 °C, two of the three NQIs (NQI-2 and NQI-3 in Tables IV and V) together account for about 50% of the spectral intensity. This suggests that in the complex of *R*-thiomandelate with the binuclear cadmium enzyme, one of the two metal sites exists in an equilibrium between two coordination geometries that interconvert with a rate sufficiently slow at −20 °C to produce two static NQIs. In agreement with this hypothesis, the spectrum at 30 °C can be explained by the sum of only two NQIs, each accounting for ~50% of the intensity. NQI-1 at 30 °C is the same as NQI-1 at −20 °C, whereas NQI-4 at 30 °C is intermediate between NQI-2 and NQI-3 at −20 °C. This suggests that at 30 °C, the rate of interconversion between the two coordination geometries has increased to a value such that only one NQI is observed as the average of the two NQIs detected at −20 °C, making an interesting PAC analogue of the effects of chemical exchange in NMR. Note that the fitted value of ω_0 for NQI-4, from the 30 °C spectrum, is identical to the numerical average of the fitted values for NQI-2 and NQI-3 from the −20 °C spectrum. At 1 °C, the rate appears to be in an "intermediate exchange" range, and the spectrum could be fitted as a broadening of the average NQI fitted at 30 °C. In addition to these dynamic complexities, the spectra in Fig. 8 demonstrate that, for the complexes of *R*-thiomandelate as for those of *S*-thiomandelate discussed above, weak new features appear at low metal ion stoichiometry, which we attribute to one or more species of the mononuclear complex.

TABLE II
NQIs observed with ^{111m}Cd BcII β-lactamase in the presence of equimolar amounts of the inhibitor S-thiomandelate

Samples contained 0.5 mM BcII + 0.5 mM *S*-thiomandelate; spectra were obtained at 1 °C.

	ω_0	η	δ^a	$\tau_R{}^a$
	megarads/s			*ns*
NQI-1	115.4 ± 0.7	0.847 ± 0.010	0.064 ± 0.004	278 ± 23
NQI-2	187.4 ± 1.0	0.641 ± 0.010	0.064 ± 0.004	278 ± 23
NQI-3	92.9 ± 5.6	0.873 ± 0.119	0.064 ± 0.004	278 ± 23
NQI-4	171.0 ± 2.2	0.712 ± 0.021	0.064 ± 0.004	278 ± 23

[a] The fit was performed assuming equal values of δ and τ_R for all NQIs.

TABLE III
Occupancy of different metal sites in BcII β-lactamase as observed with ^{111m}Cd PAC in the presence of equimolar amounts of the inhibitor S-thiomandelate

Samples contained 0.5 mM BcII + 0.5 mM *S*-thiomandelate; see "Experimental Procedures" for conditions.

[Cd(II)]/[Enzyme]	Percentage occupancy[a]		
	0.01	0.2	1.9
NQI-1	32 ± 3	41 ± 3	50[b]
NQI-2	32[c]	41[c]	50[b]
NQI-3	8 ± 3	−3 ± 2	0[b]
NQI-4	28 ± 4	20 ± 4	0[b]
χ^2 (overall 1.24)	1.15	1.30	1.14

[a] The occupancy is given by the amplitude of each component signal (NQI_i) as a percentage of the total signal amplitude (NQI_t).
[b] Only two NQIs observervable; the amplitudes of NQI-1 and NQI-2 were each assumed to be equal to 50%.
[c] Amplitudes of NQI-2 assumed equal to those of NQI-1.

DISCUSSION

Resistance to β-lactam antibiotics mediated by metallo-β-lactamases is an increasing problem, and as yet no satisfactory inhibitor is available for clinical use. Candidate inhibitors include mercaptocarboxylic acids, and we have recently shown (23) that a simple such compound, thiomandelic acid, is a broad spectrum inhibitor of MBLs, with a submicromolar K_i for eight of the nine enzymes tested. The K_i values for the dizinc BcII enzyme are 0.09 μM for *R*-thiomandelic acid and 1.28 μM for the *S*-isomer. Structure-activity relationships showed that the thiol is essential for activity and that the carboxylate increases potency. We proposed that the inhibitor thiol binds to both zinc ions, as observed for a much larger mercaptocarboxylate binding to the IMP-1 enzyme (16), whereas its carboxylate binds to Arg^{91}.

The NMR data reported in the present paper provide unequivocal evidence that *R*-thiomandelate indeed binds through its thiolate sulfur to both the metal ions in the cadmium-substituted enzyme. The observation in the ^{1}H,^{113}Cd HMQC spectrum of cross-peaks from both cadmium signals to the resonance of the α-proton of *R*-thiomandelate, together with the quartet structure of this proton resonance, demonstrates that each cadmium has a molecule of *R*-thiomandelate bound to it. The results of the selective cadmium decoupling experiment demonstrate clearly that a single *R*-thiomandelate α-proton is scalar coupled to both cadmiums and hence that a single *R*-thiomandelate molecule binds to the enzyme, binding to both metals simultaneously. The inhibitor clearly binds to the metals through its sulfur, as demonstrated by the very large (up to 200 ppm) downfield shift of the ^{113}Cd resonances on inhibitor binding, characteristic of sulfur coordination, and by the observation of $J_{H\text{-}Cd}$ scalar couplings of 15–30 Hz, typical of three-bond couplings through the sulfur rather than the four-bond couplings that would be involved if the binding was through the inhibitor's carboxylate group.

With the information that the sulfur of *R*-thiomandelate coordinates to both cadmium ions, we attempted, as described under "Experimental Procedures," to produce a model for the complex by computationally docking the inhibitor into the crystal structure of the *B. cereus* enzyme with two zinc ions bound (8), assuming that, as for the *B. fragilis* enzyme (13), the structures of the cadmium and zinc enzymes are closely similar. Initial attempts failed to identify a low energy structure in which the inhibitor sulfur was bound to both metals. Examination of the structures obtained indicated that the side chain of Lys^{171} (BBL 224), which interacts with the carboxylate group of the inhibitor, plays a crucial role.[7] In the recent crystal structure of a mercaptocarboxylate inhibitor bound to the IMP-1 MBL (16), in which the sulfur of the inhibitor binds to both metals, the side chain of the corresponding Lys^{161} is essentially fully extended. We therefore repeated the docking calculations after changing the side chain of Lys^{171} to an extended conformation and obtained a low energy structure in which the sulfur was bound to both metals; this is shown in Fig. 10. The sulfur atom of the inhibitor is positioned essentially equidistant from the two metals, whereas one oxygen of the carboxylate group of the inhibitor forms a good hydrogen bond with the ε-NH_3^+ of Lys^{171} and the other interacts with the zinc in site 2. Docking thiomandelate into other structures where Lys^{171} is in an extended conformation (14, 16) supports this binding mode. Thus, it appears that the inhibitor displaces both water molecules bound to the metals in the free dizinc enzyme; its sulfur atom displaces the "bridging" water, whereas the carboxylate displaces the additional water (or carbonate ion in one structure) (8) bound to the metal in site 2. Whereas this is only a model (it does not, for example, reflect the changes in the β3-β4 loop on inhibitor binding) (23), it is likely that it contains some of the essential features of *R*-thiomandelate binding. Thus, in the model, Hα of the bound *R*-thiomandelate is 1.95 Å from Hε of histidine 149, and a strong nuclear Overhauser effect between these two protons is indeed observed,[8] suggesting that the position of *R*-thiomandelate relative to the metal ions shown in Fig. 10 is basically correct.

The *S*-isomer of the inhibitor also appears to bind to both metals simultaneously, although in this case the evidence, while strong, is not entirely unequivocal. Only one of the two cadmium resonances, assigned to the metal in site 2, shows a cross-peak to the thiomandelate α-proton resonance in the ^{1}H-^{113}Cd HMQC spectrum. However, the resonance from the cadmium in site 1 also shows a very large downfield shift (140 ppm) on *S*-thiomandelate binding, with the direction and magnitude expected for coordination of a sulfur atom and almost as large as that seen on the binding of *R*-thiomandelate. Further support for the idea that the sulfur of S-thiomandelate binds to both cadmium ions comes from calculations of the NQIs using the angular overlap model (AOM) (38), the results of which are

[7] These calculations indicate that our earlier suggestion (25) that the carboxylate of thiomandelate might interact with Arg^{91} is incorrect; it was not possible to find a low energy structure in which this interaction was formed, and the large change in amide NH chemical shift observed for Arg^{91} (25) must be an indirect effect, perhaps via the metal ligand Asp^{90}.

[8] C. F. Damblon, unpublished observations.

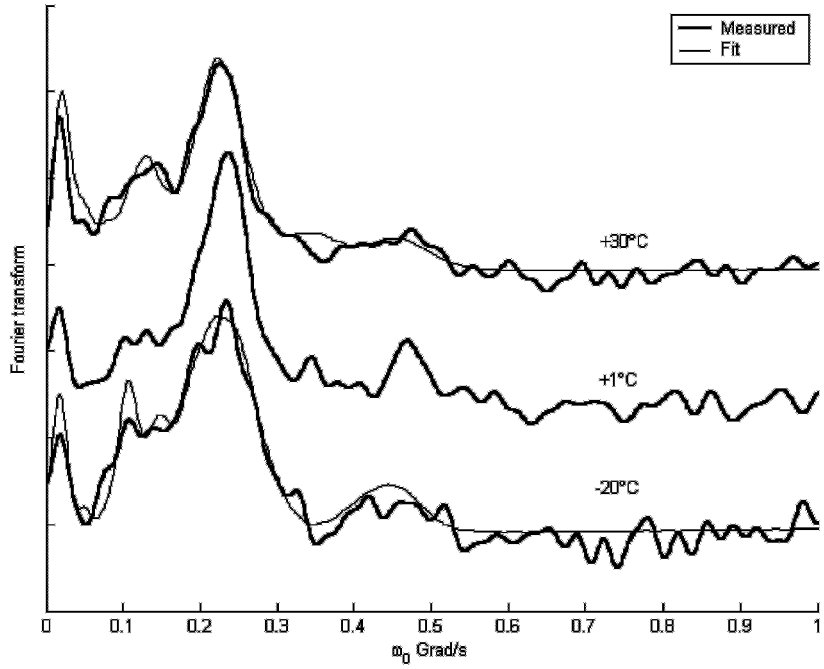

FIG. 9. **Temperature dependence of the PAC spectra of the *R*-thiomandelate complex of the dicadmium enzyme.** The sample contained enzyme, cadmium, and *R*-thiomandelate at a ratio of 1:1.9:1; spectra were recorded at temperatures of −20, 1, and 30 °C.

TABLE IV
NQIs observed with ^{111m}Cd BcII β-lactamase in the presence of equimolar amounts of the inhibitor R-thiomandelate

Samples contained 0.5 mM BcII + 0.5 mM *R*-thiomandelate, with [cadmium]/[enzyme] = 1.9; spectra were obtained at −20 and +30 °C and fitted simultaneously, assuming $\delta = 0.064$ (as for *S*-thiomandelate).

	ω_0	η
	megarads/s	
NQI-1	134.7 ± 1.1	0.844 ± 0.018
NQI-2	94.5 ± 1.9	0.349 ± 0.038
NQI-3	133.6 ± 2.4	0.303 ± 0.051
NQI-4	114.3 ± 2.6	0.346 ± 0.050

TABLE V
Occupancy of metal sites in BcII β-lactamase R-thiomandelate complex at high cadmium stoichiometry as a function of temperature

Samples contained 0.5 mM BcII + 0.5 mM *R*-thiomandelate, with [cadmium]/[enzyme] = 1.9.

	Percentage occupancy[a]	
	−20 °C[b]	+30 °C[b]
NQI-1	46 ± 4	55 ± 6
NQI-2	31 ± 3	
NQI-3	23 ± 4	
NQI-4		45 ± 5
χ^2 (overall 1.18)	1.08	1.19

[a] The occupancy is given by the amplitude of each component signal (NQI_i) as a percentage of the total signal amplitude (NQI_i).
[b] The fitted values of τ_R were 192 ± 26 ns at −20 °C and 45 ± 5 ns at +30 °C.

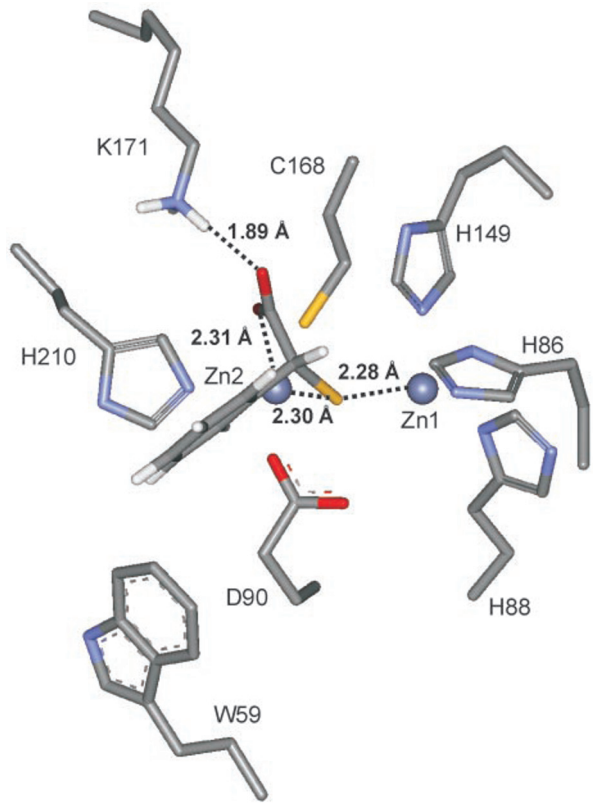

FIG. 10. **Model of the binding of *R*-thiomandelate to the active site of BcII.** See "Discussion" for the assumptions made in building the model.

shown in Fig. 11. Site 1 was modeled with tetrahedral geometry with three histidine ligands and a mercaptosulfur ligand; from Fig. 11*A* one can observe that AOM calculations for this site fit reasonably well with the NQIs with values for ω_0 of about 200 megarads/s, although η is somewhat high. Site 2 was modeled either with tetrahedral geometry with a histidine, an aspartic acid, a cysteine and a mercaptosulfur ligand (Fig. 11*B*) or with a five-coordinate geometry including a water ligand positioned opposite the histidine ligand (Fig. 11*C*). For site 2, the calculations for the five-coordinated geometry fit the data well. Thus AOM calculations support the idea that the mercaptosulfur of *S*-thiomandelate binds both cadmium ions.

We thus conclude that both isomers of this simple inhibitor bind through their sulfur atom to both cadmium atoms simultaneously. There are differences between the two isomers in their precise mode of binding, manifest in the different parameters for the cadmium NQIs derived from the PAC spectra of the two inhibitor complexes of the dicadmium enzyme, in the different ^{113}Cd chemical shifts, and in the ^{1}H and ^{15}N chemical shifts of the metal ligands. These differences most probably reflect differences in the cadmium-sulfur bond lengths and angles in the two complexes, imposed by the necessarily differ-

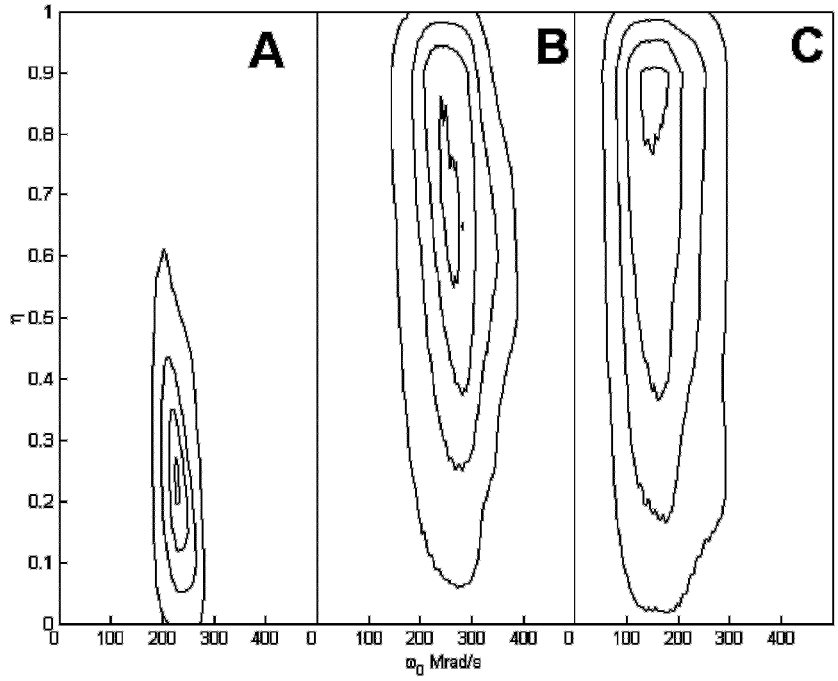

FIG. 11. **Angular overlap model calculations of NQIs in a four- or five-coordinated geometry.** The four-coordinated geometries chosen as tetrahehedral consist of either three histidine ligands and a mercaptosulfur ligand (site 1) (*A*) or a histidine, an aspartic acid, a cysteine, and a mercaptosulfur ligand (site 2) (*B*). The five-coordinated geometry, an alternative for site 2 (*C*), includes a water ligand positioned opposite the histidine ligand. Each set of polar angles for the ligands is allowed to vary up to 20° from the tetrahedral positions. The position of the fifth ligand is kept fixed. For each set of polar angles, two NQI parameters, ω_0 and η, are calculated. The frequency of occurrence weighted with the solid angle of all values of ω_0 and η is then determined and plotted in the contour plots shown.

ent interactions of the two isomers with nearby protein residues, but the chemical shifts are not sufficiently well understood to allow us to draw clear cut structural conclusions. The docking calculations for *S*-thiomandelate (not shown) suggest that for this isomer, unlike the *R*-isomer shown in Fig. 10, the carboxylate group binds to Lys[171] (BBL 224) but not to the metal in site 2, so that in this complex the fifth ligand to the cadmium in this site may be a water molecule. This difference would certainly be expected to lead to differences in cadmium and imidazole chemical shifts. The $^3J_{\text{H-Cd}}$ scalar coupling constants to the inhibitor Cα proton are notably different between the complexes with *R*-thiomandelate (15 and 31 Hz) and *S*-thiomandelate (<15 Hz). The magnitudes will depend on the orientation of the inhibitor in the complex, through the dihedral angle about the thiomandelate Cα–S bond, but also on the electron distribution on the metals and their ligands, and clear-cut relationships to conformation can rarely be discerned (25, 39). We earlier noted that the changes in backbone amide ^{1}H and ^{15}N chemical shifts on inhibitor binding to the zinc enzyme are generally very similar for the two isomers (23), suggesting that the structural differences between the two complexes are local ones.

A striking difference between the two inhibitor complexes formed with *R*- and S-thiomandelate is the observed influence of a dynamic process at one of the two metal sites on the PAC spectra of the *R*-thiomandelate complex. This was unambiguously established by the temperature dependence of the spectra but was not observed for the *S*-thiomandelate complex. This may reflect a local conformational difference between the *R*- and *S*-thiomandelate complexes such that a dynamic process occurs uniquely in the former. On the other hand, it may also be that the same process occurs in both complexes but much more rapidly (with a time constant less than 1 ns corresponding to rates of $>10^9$ s^{-1}) in the *S*-thiomandelate complex so that only an average is observed. The nature of this dynamic process cannot be identified with certainty, but some possibilities can be ruled out. First, the fact that the $^1J_{\text{H-Cd}}$ scalar couplings are observed for all of the histidine metal ligands (and cross-peaks are observed for these and for Cys[168] in the ^{1}H,^{113}Cd HMQC spectrum) in the *R*-thiomandelate complex rules out the possibility that any of these are dissociating from and reassociating to the metals at rates >90 s^{-1}, much too slow to produce dynamic effects in the PAC spectra. Furthermore, the observation of two $^3J_{\text{H-Cd}}$ scalar coupling constants of 15 and 31 Hz between the metals and the thiomandelate α-proton, together with the analysis of the PAC spectra demonstrating that only one of the two metals is affected by this dynamic process, rules out the possibility that the thiol group of the inhibitor is "jumping" between the two metals at >10 s^{-1}. One possibility is that it arises from the dissociation and reassociation of the carboxylate group of the inhibitor, which our modeling suggests binds to the cadmium in site 2 in the *R*-thiomandelate complex but not in that of the *S*-isomer. Comparison of the results of the AOM calculations for site 2 in Fig. 11, *B* and *C*, illustrates the change in the frequency parameter ω_0 that would arise from such an exchange of an oxygen ligand. However, this simple model does not account quantitatively for the measured NQIs of the *R*-thiomandelate-enzyme complex, indicating that other changes in the coordination sphere must occur in this dynamic process.

One of the most striking observations in the present work is the clear demonstration of positive cooperativity in metal binding in the presence of either isomer of the inhibitor. We have recently demonstrated that in the absence of the inhibitor there is negative cooperativity in cadmium binding to BcII from strain 569/H/9 (24). The two macroscopic dissociation constants for cadmium binding differ by a factor of ~1000 (26), but at [cadmium]/[enzyme] < 1, the PAC spectra show that the metal occupies two sites with roughly equal probability. Thus, the two macroscopic constants do not reflect metal binding to two distinct sites with different intrinsic affinities but rather reflect negative cooperativity in metal binding in the absence of inhibitor. Studies of the wild-type and mutant enzyme by optical spectroscopy and extended x-ray absorption fine structure experiments indicated that there is a similar negative cooperativity in the binding of zinc and cobalt to the enzyme (40). However, the present experiments demonstrate that in the presence of the inhibitor thiomandelate there is positive cooperativity in cadmium binding. NMR experiments carried out at an enzyme/cadmium/inhibitor ratio of 1:1:1 demonstrated that the sample contained an approximately equimolar mixture of the inhibitor complex of the binuclear cadmium enzyme and

apoenzyme. These were clearly identified from their characteristic $^{1}H,^{15}N$ HSQC spectra, which also showed that any other species, such as enzyme with only one cadmium bound, represented ≤5% of the enzyme. These observations cannot be explained by equal macroscopic dissociation constants for binding the two cadmium ions in the presence of the inhibitor. PAC spectra were obtained over a wide range of [cadmium]/[enzyme] ratios in the presence of *S*-thiomandelate, and analysis of these spectra showed that even at a [cadmium]/[enzyme] ratio as low as 0.01, the binuclear cadmium enzyme represented 64% of the total cadmium present, again inconsistent with equal K_d values for the two metals and indicating a marked cooperativity in metal binding. The observed relative amounts of mono- and binuclear cadmium species as a function of [cadmium]/[enzyme] ratio (from 0.01 to 2.0) can only be satisfactorily simulated by a macroscopic dissociation constant for the binding of one cadmium ion about 100-fold greater than that for the binding of the second cadmium ion. The observed positive cooperativity clearly results from the fact that the inhibitor coordinates simultaneously to both metals, and one would thus expect a similar cooperativity with the physiological metal zinc, although direct measurements of this do not exist.

Recent measurements suggest that at physiological metal ion concentrations, most metallo-β-lactamases may exist as the apoenzyme and that the presence of substrate leads to enhanced zinc binding in the mononuclear form of the enzyme (41). The present experiments suggest a parallel in the sense that the addition of the inhibitor markedly changes the relative populations of the mono- and binuclear enzyme forms. Depending on the metal concentration in the milieu in which the enzyme exists (*cf.* Ref. 41), the requirement for two metal ions for optimal inhibitor binding might be considered a disadvantage of this class of inhibitors for clinical applications. However, the existence of marked inhibitor-induced cooperativity in metal ion binding that we have demonstrated here means that, even at low metal concentrations, the binuclear enzyme will be a substantial proportion of the total, and the catalytic activity will be effectively inhibited by converting the mononuclear enzyme into a mixture of inhibited binuclear enzyme and inactive apoenzyme.

Acknowledgments—We acknowledge Eva Danielsen for helpful suggestions and discussions concerning the dynamic PAC effects under the influence of a rapidly exchanging carboxyl group. We thank the cyclotron department at Copenhagen University Hospital for ever punctual assistance with the cyclotron irradiations. In addition, we are indebted to Marianne Lund Jensen for excellent laboratory work.

REFERENCES

1. Frere, J. M. (1995) *Mol. Microbiol.* **16,** 385–395
2. Wang, Z., Fast, W., Valentine, A. M., and Benkovic, S. J. (1999) *Curr. Opin. Chem. Biol.* **3,** 614–622
3. Kuwabara, S., and Abraham, E. P. (1967) *Biochem. J.* **103,** 27C-30C
4. Laraki, N., Franceschini, N., Rossolini, G. M., Santucci, P., Meunier, C., de Pauw, E., Amicosante, G., Frere, J. M., and Galleni, M. (1999) *Antimicrob. Agents Chemother.* **43,** 902–906
5. Payne, D. J. (1993) *J. Med. Microbiol.* **39,** 93–99
6. Carfi, A., Pares, S., Duee, E., Galleni, M., Duez, C., Frere, J. M., and Dideberg, O. (1995) *EMBO J.* **14,** 4914–4921
7. Carfi, A., Duee, E., Paul-Soto, R., Galleni, M., Frere, J. M., and Dideberg, O. (1998) *Acta Crystallogr. D Biol. Crystallogr.* **54,** 45–57
8. Carfi, A., Duée, E., Galleni, M., Frère, J. M., and Dideberg, O. (1998) *Acta Crystallogr.* **D54,** 313–323
9. Concha, N. O., Rasmussen, B. A., Bush, K., and Herzberg, O. (1996) *Structure* **4,** 823–836
10. Fabiane, S. M., Sohi, M. K., Wan, T., Payne, D. J., Bateson, J. H., Mitchell, T., and Sutton, B. J. (1998) *Biochemistry* **37,** 12404–12411
11. Fitzgerald, P. M., Wu, J. K., and Toney, J. H. (1998) *Biochemistry* **37,** 6791–6800
12. Ullah, J. H., Walsh, T. R., Taylor, I. A., Emery, D. C., Verma, C. S., Gamblin, S. J., and Spencer, J. (1998) *J. Mol. Biol.* **284,** 125–136
13. Concha, N. O., Rasmussen, B. A., Bush, K., and Herzberg, O. (1997) *Protein Sci.* **6,** 2671–2676
14. Toney, J. H., Fitzgerald, P. M., Grover-Sharma, N., Olson, S. H., May, W. J., Sundelof, J. G., Vanderwall, D. E., Cleary, K. A., Grant, S. K., Wu, J. K., Kozarich, J. W., Pompliano, D. L., and Hammond, G. G. (1998) *Chem. Biol.* **5,** 185–196
15. Paul-Soto, R., Zeppezauer, M., Adolph, H. W., Galleni, M., Frere, J.-M., Carfi, A., Dideberg, O., Wouter, J., Hemmingsen, L., and Bauer, R. (1999) *Biochemistry* **38,** 16500–16506
16. Concha, N. O., Janson, C. A., Rowling, P., Pearson, S., Cheever, C. A., Clarke, B. P., Lewis, C., Galleni, M., Frere, J. M., Payne, D. J., Bateson, J. H., and Abdel-Meguid, S. S. (2000) *Biochemistry* **39,** 4288–4298
17. Galleni, M., Lamotte-Brasseur, J., Rossolini, G. M., Spencer, J., Dideberg, O., and Frere, J. M. (2001) *Antimicrob. Agents Chemother.* **45,** 660–663
18. Orellano, E. G., Girardini, J. E., Cricco, J. A., Ceccarelli, E. A., and Vila, A. J. (1998) *Biochemistry* **37,** 10173–10180
19. Crowder, M. W., Walsh, T. R., Banovic, L., Pettit, M., and Spencer, J. (1998) *Antimicrob. Agents Chemother.* **42,** 921–926
20. Wang, Z., and Benkovic, S. J. (1998) *J. Biol. Chem.* **273,** 22402
21. Bounaga, S., Laws, A. P., Galleni, M., and Page, M. I. (1998) *Biochem. J.* **331,** 703–711
22. Paul-Soto, R., Bauer, R., Frere, J. M., Galleni, M., Meyer-Klaucke, W., Nolting, H., Rossolini, G. M., de Seny, D., Hernandez-Valladares, M., Zeppezauer, M., and Adolph, H. W. (1999) *J. Biol. Chem.* **274,** 13242–13249
23. Mollard, C., Moali, C., Papamicael, C., Damblon, C., Vessilier, S., Amicosante, G., Schofield, C. J., Galleni, M., Frere, J. M., and Roberts, G. C. K. (2001) *J. Biol. Chem.* **276,** 45015–45023
24. Hemmingsen, L., Damblon, C., Antony, J., Jensen, M., Adolph, H. W., Wommer, S., Roberts, G. C. K., and Bauer, R. (2001) *J. Am. Chem. Soc.* **123,** 10329–10335
25. Damblon, C., Prosperi, C., Lian, L. Y., Barsukov, I., Paul-Soto, R., Galleni, M., Frère, J. M., and Roberts, G. C. K. (1999) *J. Am. Chem. Soc.* **121,** 11575–11576
26. Piotto, M., Sudiek, V., and Sklenar, V. (1992) *J. Biomol. NMR* **2,** 661–665
27. Kuboniwa, H., Grzesiek, S., Delaglio, F., and Bax, A. (1994) *J. Biomol. NMR* **4,** 871–878
28. McCoy, M. A., and Mueller, L. (1992) *J. Magn. Reson. A* **101,** 122–130
29. Hemmingsen, L., Bauer, R., Bjerrum, M. L., Zeppezauer, M., Adolph, H. W., Formicka, G., and Cedergren-Zeppezauer, E. (1996) *Eur. J. Biochem.* **241,** 546–551
30. Bauer, R., Danielsen, E., Hemmingsen, L., Sorensen, M. V., Ulstrup, J., Friis, E. P., Auld, D. S., and Bjerrum, M. J. (1997) *Biochemistry* **36,** 11514–11524
31. Bauer, R., Danielsen, E., Hemmingsen, L., Bjerrum, M. J., Hansson, O., and Singh, K. (1997) *J. Amer. Chem. Soc.* **119,** 157–162
32. Bauer, R. (1985) *Q. Rev. Biophys.* **18,** 1–64
33. Cornell, W. D., Cieplak, P., Bayly, C. I., Gould, I. R., Merz, Jr., K. M., Ferguson, D. M., Spellmeyer, D. C., Fox, T., Caldwell, J. W., and Kollman, P. A. (1995) *J. Amer. Chem. Soc.* **117,** 5179–5197
34. Dixon, S. L., and Merz, K. M., Jr. (1997) *J. Chem. Phys.* **107,** 879–893
35. Gogonea, V., and Merz, K. M., Jr. (1999) *J. Phys. Chem. A* **103,** 5171–5188
36. Morris, G. M., Goodsell, D. S., Halliday, R. S., Hart, W. E., Belew, R. K., and Olson, A. J. (1998) *J. Comp. Chem.* **19,** 1639–1662
37. Hanessian, S., Mitessier, N., Therrien, E. (2001) *J. Comp.-Aided Mol. Design* **15,** 673–881
38. Bauer, R., Jensen, S. J., and Nielsen, B. S. (1988) *Hyperfine Interact.* **39,** 203–234
39. Baleja, J. D., Thanabal, V., and Wagner, G. (1997) *J. Biomol. NMR* **10,** 397–401
40. de Seny, D., Heinz, U., Wommer, S., Kiefer, M., Meyer-Klaucke, W., Galleni, M., Frere, J. M., Bauer, R., and Adolph, H. W. (2001) *J. Biol. Chem.* **276,** 45065–45078
41. Wommer, S., Rival, S., Heinz, U., Galleni, M., Frere, J.-M., Franceschini, N., Amicosante, G., Rasmussen, B., Bauer, R., and Adolph, H.-W. (2002) *J. Biol. Chem.* **277,** 24142–24147